Journal of Structural Geology, Vol. 8, No. 2, pp. 111 to 122, 1986
Printed in Great Britain

0191-8141/86 $03.00 + 0.00

Asymmetrical pull-aparts and foliation fish as kinematic indicators

SIMON HANMER

Geological Survey of Canada, 588 Booth St, Ottawa, Ontario, K1A 0E4, Canada

(*Received* 14 *January* 1985; *accepted in revised form* 21 *June* 1985)

Abstract—From field observations, asymmetrical boudins, pinch-and-swell structures and ellipsoidal volumes of oblique foliation segments in anisotropic rocks lacking competent layers are potentially useful kinematic indicators in shear zones. They are derived by the modification of initially symmetrical pull-aparts and/or layering by superposed layer-parallel shearing. The response of boudins to such shear is a synthetic flow of those corner volumes lying within the extensional quadrants of the kinematic framework of the deformation into the inter-boudin gaps (Type 1 asymmetrical pull-aparts). The response of pinch-and-swell structure is a back-rotation of the 'swells' to form Type 2 asymmetrical pull-aparts. Discrete extensional shears in the 'pinches' may be either absent (Type 2A) or present (Type 2B). Analogues of Types 2A and 2B asymmetrical pull-aparts occur in anisotropic materials with no compositionally distinct competent members where ellipsoidal volumes contain back-rotated foliation segments (foliation fish).

The field-based kinematic interpretation was successfully tested by laboratory experiment wherein initially symmetrical trains of pre-formed competent, internally anisotropic boudins and pinch-and-swell structures were deformed in bulk simple shear. A mechanical model is presented in terms of two material properties of the inclusions (competence/viscosity and internal rheological anisotropy) in an attempt to account for the observed flow in the experiments and the deduced flow and kinematic significance of the natural examples. In the presence of angular corners and associated geometrical stress concentrations, competence/viscosity controls the response to shear in the boudins. In the absence of angular corners, internal anisotropy controls the response to shear in the pinch-and-swell structures and in the foliation fish.

INTRODUCTION

ASYMMETRICAL pull-apart structures (some types of boudins and pinch-and-swell structures) and ellipsoidal volumes of oblique foliation segments in anisotropic rocks lacking competent layers are potentially useful kinematic indicators in highly deformed rocks such as those found in shear zones, if a reasonable model for their formation can be proposed. Pull-apart structures may be particularly useful in high grade metamorphic terranes which have undergone secondary recrystallization (Hobbs *et al.* 1976, p. 113), where other, more delicate indicators (e.g. crystallographic preferred orientations, composite foliations, pressure shadows, etc.) may not be preserved.

Symmetrical pull-apart structures in layered rocks fall naturally into two, kinematically similar, but mechanically distinct types: boudins and pinch-and-swell structure (e.g. Smith 1975, 1977, 1979, Lloyd & Ferguson 1981, Lloyd *et al.* 1982, Neurath & Smith 1982). "Boudin" and the related term "boudinage" were introduced by Lohest (1909) and have sometimes been indiscriminately applied to a variety of pull-aparts and "tectonic inclusions" (Rast 1956). This has perhaps contributed to both culinary (Wilson 1982, p. 72) and kinematic confusion. Although now accepted as an indicator of apparent instantaneous extension within the layering (Corin 1931, Wegmann 1932, Sanderson 1974), pull-apart structure has been interpreted by some authors in terms of layer-parallel shortening (Harker 1889, Lohest 1909, Quirke 1923, Holmquist 1931, Bruhl 1967). This stems, in part from the misconception (Corin 1931) that the barrel shape of some pull-aparts represents a real increase in layer thickness, and in part from a confusion between mullion and pull-apart structures (e.g. Dearman 1966).

The mechanics of symmetrical boudinage have been illustrated by numerous studies involving physical and numerical modelling (Ramberg 1955, Paterson & Weiss 1968, Strömgård 1973, Selkman 1978, Lloyd & Ferguson 1981, Lloyd *et al.* 1982) and by comparisons with similar phenomena in metallurgy (Rast 1956, Talbot 1970, Burg & Harris 1982). The dynamics of pinch-and-swell structure (flow boudinage) have been examined by Smith (1975, 1977, 1979), Fullagar (1980) and Neurath & Smith (1982). All of these studies were concerned with the initiation and/or the evolution of symmetrical pull-apart structures. The present paper is concerned with the asymmetrical evolution of such initially symmetrical structures in response to an imposed layer-parallel shearing deformation.

With respect to shearing deformation, *a kinematic indicator is a structure, resulting from flow, whose geometry is indicative of the progressive rotation of the principal axes of finite strain with respect to the principal axes (stretches) of the kinematic framework and/or the shear plane of the deformation*; more simply it is indicative of the sense of flow. This definition requires a mechanical model of progressive strain from which the kinematic significance of the geometry of the specific structure in question may be deduced. For example, if the asymmetrical tails attached to a feldspar porphyroclast have formed by flow of material into a pressure

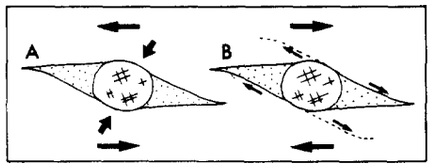

Fig. 1. Schematic illustration of the dependence of kinematic significance upon mechanical model proposed to account for geometry in the case of a porphyroclast, such as a feldspar, with asymmetrical polycrystalline tails (dotted). (a) If the tails form by flow of material into the pressure shadows (short arrows = direction of instantaneous maximum shortening) the sense of shear deduced is opposite to that given (b) if geometrically identical tails form by flow along oblique extensional shears (for example components of shear band foliation). Small arrows indicate local shear sense.

shadow they will indicate the opposite sense of flow to geometrically similar tails formed by flow along oblique extensional shears located adjacent to the porphyroclast (Fig. 1). The onus is upon the observer to propose a testable mechanical hypothesis to account for the geometry of the structure to which a kinematic significance is to be attached. Examples are given by Rosenfeld (1970), Ramsay & Graham (1970), Durney & Ramsay (1973), Reches & Johnson (1976), Lister & Price (1978), Berthé *et al.* (1979), Platt & Vissers (1980), White *et al.* (1980), Means (1981), Simpson (1983) and Hanmer (1982, 1984a, 1985). Means *et al.* (1980) and Lister & Williams (1983) give a wider ranging discussion of this subject.

This paper proposes a field-based kinematic interpretation of natural asymmetrical pull-apart structures, and their analogues in anisotropic rocks lacking competent layers, to test this interpretation in the laboratory and to propose a mechanical model to account for the kinematic significance of the observed geometry.

FIELD OBSERVATIONS

Asymmetrical pull-aparts and similar structures (see below) have been observed by the author in the course of recent structural mapping in the Canadian Shield (Fig. 2) in (1) high grade (amphibolite to granulite facies) gneisses of the western Grenville Province (Wynne-Edwards 1972, Davidson *et al.* 1982) and (2) at the boundary of the western Churchill and Slave provinces (see Reinhardt 1969). In the first area, the western Grenville rocks comprise a ductile northwestward overthrust stack of laterally discontinuous tectonic slices (Davidson *et al.* 1982, Culshaw *et al.* 1983, Hanmer 1984b, Hanmer & Ciesielski 1984, Hanmer *et al.* 1985). In the second area, the boundary is the site of a major crustal-scale dextral transcurrent shear zone (Hanmer & Lucas 1985). In both field areas, independent shear-sense indicators support the interpretation of asymmetrical pull-aparts which will be presented in this paper (Figs. 2b & c).

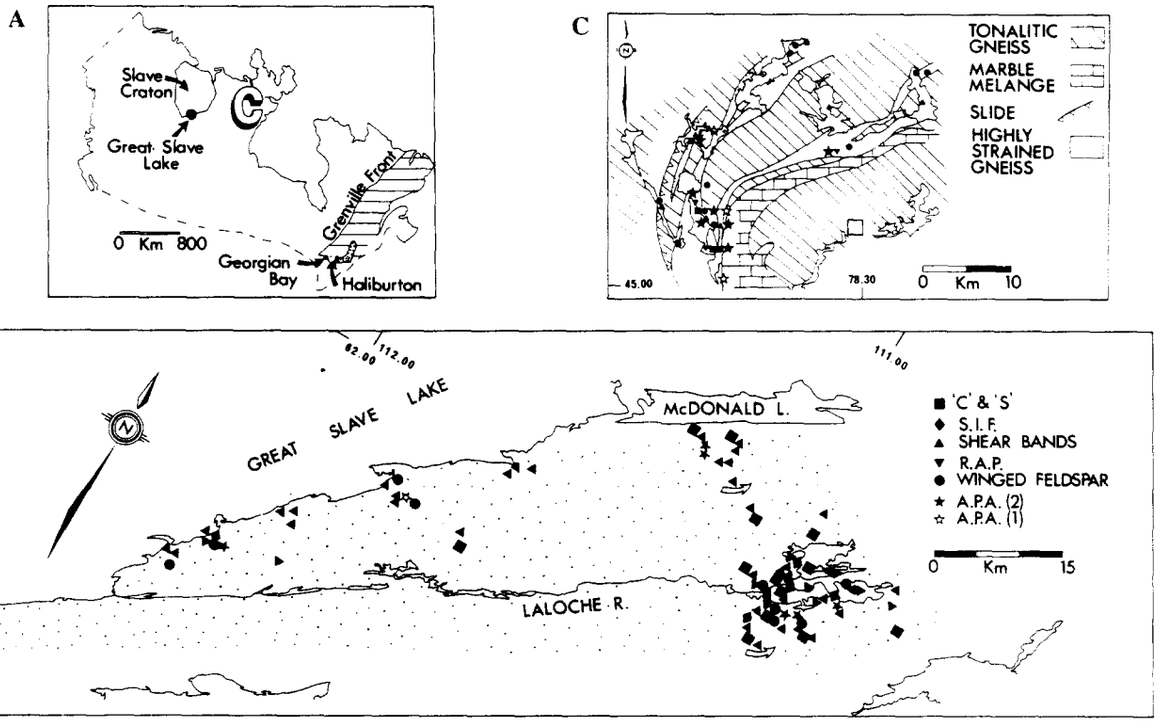

Fig. 2. (a) Location map. Western Churchill Province (C), Central Metasedimentary Belt (dotted), Grenville Province (ruled). (b) Southeast shore of Great Slave Lake is the site of a NE–SW striking crustal scale dextral shear zone (dotted). Distribution of observed assemblage of kinematic indicators, all dextral except two arrowed occurrences. C & S = 'C/S' fabrics (Berthé *et al.* 1979); S.I.F. = strain insensitive foliation (Means 1981, Hanmer 1985); R.A.P. = progressively rotated fold axial planes; A.P.A. = asymmetrical pull-aparts of Type 1 and Type 2 (including foliation fish). See text. (c) Detail of the boundary zone of the northwestward-overthrust Central Metasedimentary Belt in the Haliburton (square) region. SE-dipping slices of tonalitic gneiss are separated by marble tectonic mélange and belts of highly strained quartzo-feldspathic porphyroclastic and transposed gneisses carrying an assemblage of kinematic indicators (symbols as in b). The highly strained gneiss belts are zones of ductile shear and the kinematic indicators show consistent hanging-wall northwestward movement.

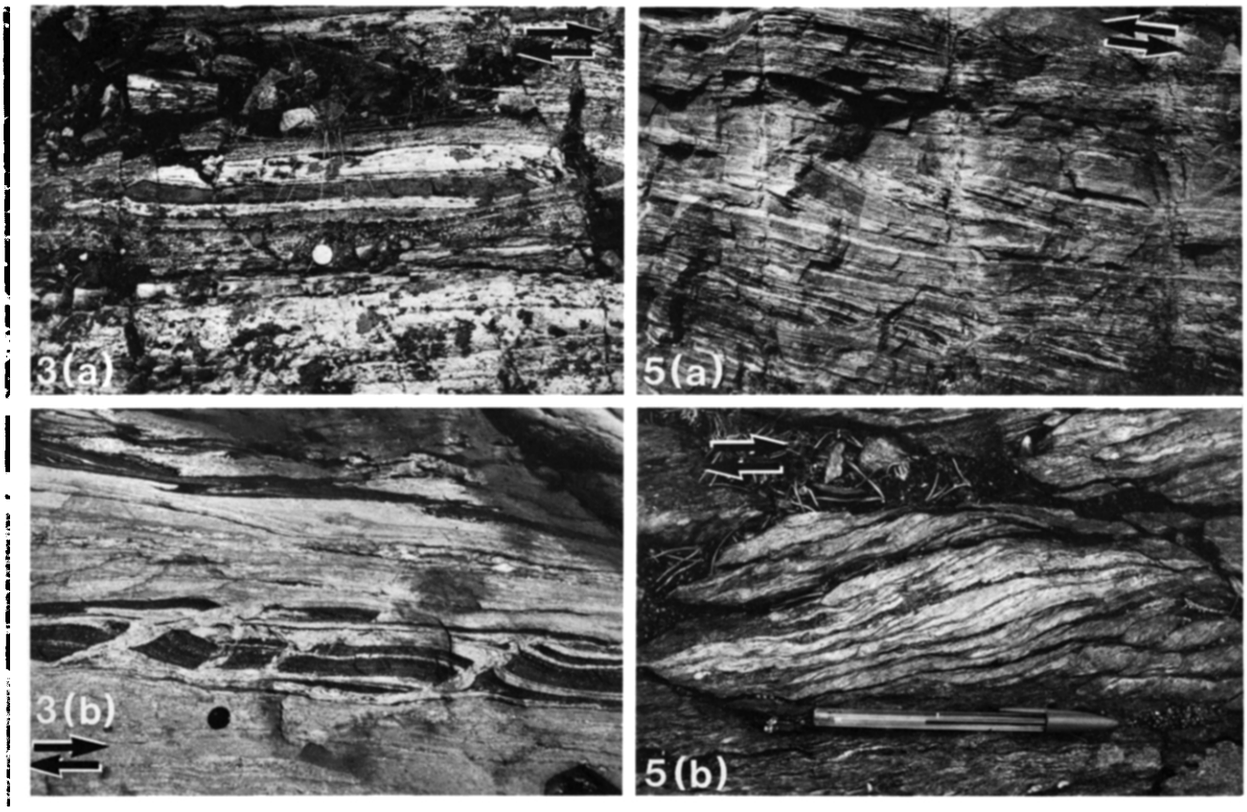

Fig. 3. (a) Detail of a single Type 1 asymmetrical pull-apart, Great Slave Lake shear zone. Coin for scale. (b) Train of Type 1 asymmetric pull-aparts; note sub-equant dextrally rotated boudin, Georgian Bay. Lens cap for scale.

Fig. 5. Foliation fish with layering parallel to the bulk shear plane. (a) Approximately ellipsoidal or spindle shaped volume of quartzo-feldspathic gneiss containing oblique internal layering/foliation (centre) set in matrix of identical composition. Note absence of discrete extensional shears at 'fish' ends, and Type 2B asymmetrical pull-aparts in lower field. Looking to the NE, near Haliburton. Outcrop 3 m high. (b) Homogeneous mylonite. The foliation both within and outside the elliptical fish (above pen) is a composite structure comprising discrete shear and penetrative flattening sub-fabrics, a strain insensitive (Means 1981, Hanmer 1984a) analogue of 'C & S' planes (Berthé *et al.* 1979). The angular relationships and sigmoidal configuration of the sub-fabrics and the incipient shear band structures (below pen) suggest bulk dextral shear. The discrete shear planes outside the 'fish' are parallel to the bulk shear plane below and to the right of the pen. Within the main 'fish' and at the end of a second one (top right) the discrete shear planes are 10–15 degrees oblique to their external continuations. The quantitatively estimated strain magnitude (degree of mylonitization from coarse granite protolith) within the 'fish' is indistinguishable from that of the external mylonite. Assuming that the discrete shear planes were initially parallel to the bulk shear plane, the foliation fish has undergone 10–15 degrees anticlockwise rotation. Great Slave Lake shear zone. The simple fabric of (a) is commoner than the complex fabrics of (b).

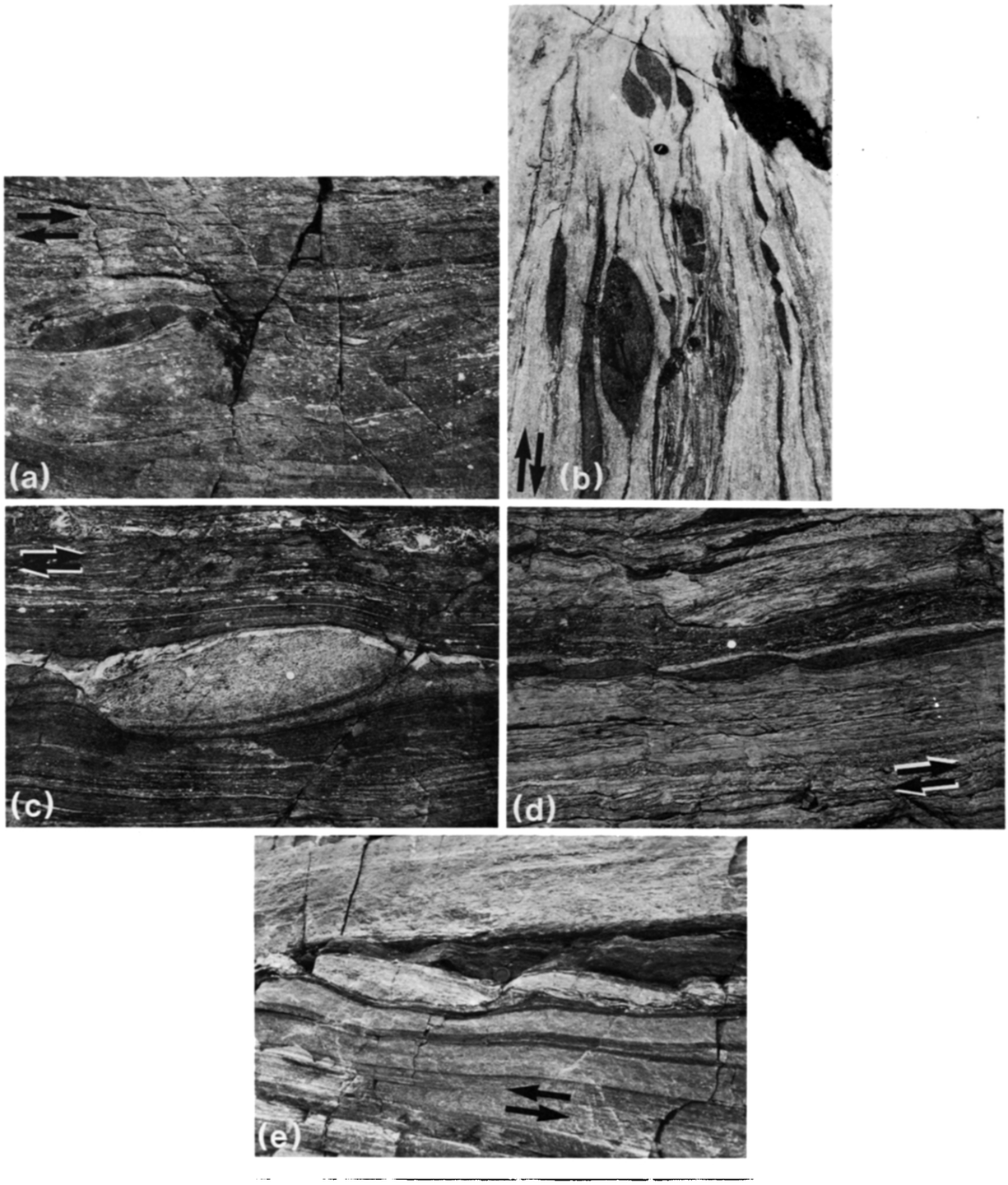

Fig. 4. Type 2 asymmetrical pull-aparts, Great Slave Lake shear zone unless indicated. Coins or lens cap for scale. *Type 2A*. (a) Two amphibolite 'swells' oblique to layering in quartzo-feldspathic protomylonite are part of a larger train. Note absence of discrete oblique extensional shear between 'swells'. (b) 'Nest' of internally foliated amphibolite 'swells' systematically oblique to layering in quartzo-feldspathic protomylonite. Note absence of discrete extensional shears except to the right. (c) Detail of similar structure to (b). Note internal oblique foliation and absence of discrete extensional shears at either end of 'swell'. *Type 2B*. (d) Part of a train of oblique amphibolite 'swells' in quartzo-feldspathic protomylonite. Note discrete extensional shears in 'pinches'. (e) Foliated oblique granitic 'swells' in biotite schist horizon in very straight gneiss. Note oblique discrete extensional shears in 'pinches'. Looking to the NE, near Haliburton.

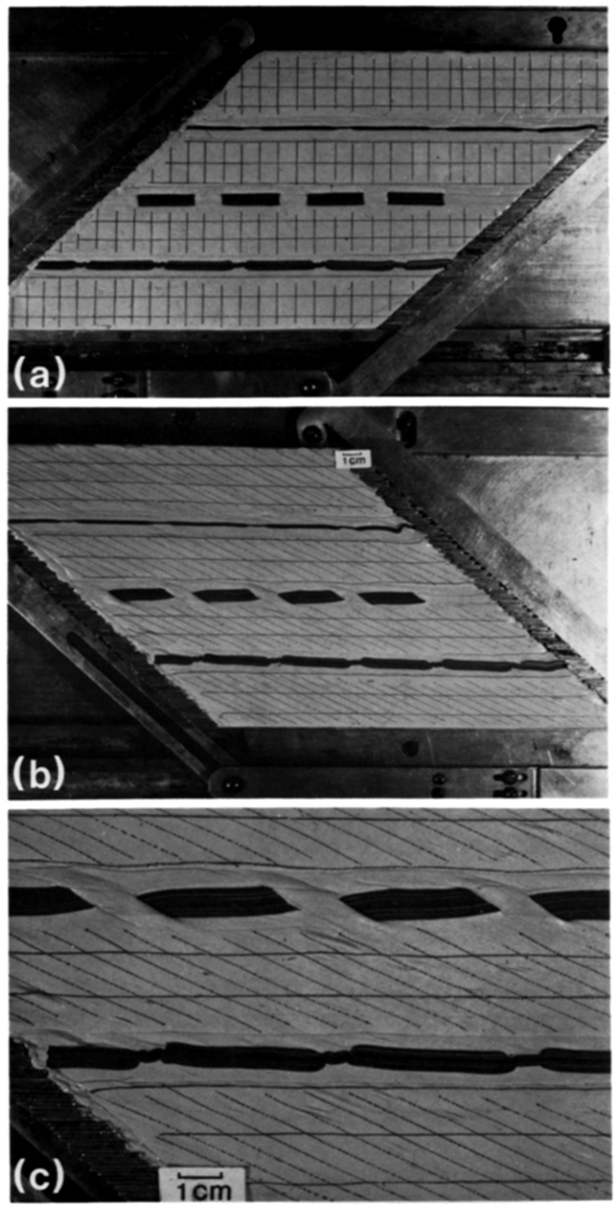

Fig. 6. Plasticine–silicone putty inserts in silicone putty matrix. Model subjected to a sinistral shear strain of 2 gamma in these pictures. (a) Initial configuration, rectangular grid of passive marker lines. (b) After deformation. (c) A detail of (b). Note slight deflections of the free-surface topography and very local heterogeneity in bulk flow (top right). See text.

Two classes (Types 1 and 2) of asymmetrical pull-aparts are distinguished, Type 2 being further subdivided (Types 2A and 2B). Structures analogous to Type 2 pull-aparts occur in anisotropic rocks lacking competent layers.

All descriptions in this paper pertain to sections normal to the axis of rotation of the non-coaxial component of the deformation. The term 'internal layering' will be used here to designate a multilayering or rheological anisotropy within heterogeneously extended competent layers or segments of oblique foliation in anisotropic rock without competent layers. The term 'bulk layering' designates the larger scale layering or foliation. All illustrations from the Great Slave Lake shear zone are views of horizontal surfaces. Those from the Grenville are views of vertical surfaces with the camera looking towards the NE, unless indicated otherwise.

Type 1 asymmetrical pull-aparts

These structures are often associated with classical boudins, that is discrete rectangular blocks derived by heterogeneous layer-parallel extension of rheologically competent, once continuous layers. The pull-aparts are generally amphibolitic in composition and set in a matrix of either granitic or more general quartzo-feldspathic gneiss (Fig. 3a). The syn-tectonic metamorphic mineral assemblages in the study areas (biotite–sillimanite–K feldspar–garnet–quartz and two feldspar–quartz–biotite–orthopyroxene) indicate deformation under upper amphibolite to lower granulite facies conditions. The rheological contrast between the amphibolite and the quartzo-feldspathic matrix material is variable. In general, thinner amphibolite layers have extended homogeneously and show no sign of having behaved more competently than their enclosing matrix, whereas intercalated thicker amphibolite layers have boudinaged (Fig. 3a). Flow of the fine-scale layering of the matrix around the already separated pull-aparts attests to the persistence of the rheological contrast.

The asymmetry of the pull-aparts is manifested at the ends of individual blocks as an asymmetrical barrelling of the block (Ramberg 1955). Internal layering and foliation, when present, are sigmoidal (Fig. 3). The sigmoid configuration comprises a straight central segment, wherein the long sides of the block and the internal layering/foliation are parallel to the bulk layering, plus curved segments at each end where the long sides and the internal layering lie at a distinct angle to the bulk layering. The curved segments occur in opposite quadrants of the block and may develop as subdued acute-angled corners or may form flamboyant, horn-like extensions. Individual equant blocks show a rigid body rotation in a sense consistent with the sigmoidal configuration of the non-rotated, markedly inequant, blocks (Fig. 3b).

Type 2 asymmetrical pull-aparts

In contrast to the Type 1 structures, Type 2 asymmetrical pull-aparts may be associated with pinch-and-swell structures developed in competent layers (Fig. 4). As in the case of Type 1 pull-aparts, these structures develop in layers of amphibolitic composition, but they are also commonly developed in quartzo-feldspathic sheets (Fig. 4e). In both cases, the 'swells' are enclosed by less competent quartzo-feldspathic material whose finer scale layering flows around the 'swells'. However, it will be suggested below that the presence of a rheological anisotropy rather than a compositionally distinct competent member is the necessary pre-condition for the development of Type 2 structures. Therefore, the designation Type 2 asymmetrical pull-apart will be reserved for those structures involving a heterogeneously extended (pinch-and-swell) competent layer, while the term 'foliation fish' will be used to designate certain analogous structures occurring in anisotropic rocks without competent layers, such as schists and mylonites (Fig. 5). In both cases, the general geometry is that of fish-shaped ellipsoidal volumes, whose internal foliation and/or layering lies oblique (at about 10 degrees) to the enclosing external planar fabric. The sense of asymmetry in a population of spatially associated Type 2 structures is consistent.

There are two sub-classes of Type 2 asymmetrical pull-aparts. In Type 2A pull-aparts (Figs. 4a–c), the orientation of the oblique internal foliation is constant within the ellipsoidal volume, except at the ends where the foliation deflects into the plane of the external bulk layering (Fig. 4b). Both the principal plane of the shape of the ellipsoidal volume and the internal foliation lie oblique to the bulk layering in the same sense (Fig. 4c). At the ends of Type 2B asymmetrical pull-aparts, the 'swells' and their internal foliation both deflect into a single set of discrete-to-zonal asymmetrical extensional shears, consistently oriented at less than 30 degrees to the external foliation (Figs. 4d & e). The sense of displacement on the extensional shears is opposite to the sense of obliquity of the 'swells'. Foliation fish are analogues of Type 2A structures occurring in schists and mylonites lacking competent layers (Fig. 5).

Where Type 2B asymmetrical structures are associated with pinch-and-swell extension of competent layers, the extensional shears lie in the 'pinches' and the volumes of oblique internal foliation correspond to the 'swells'. Analogous structures occur in schists and mylonites without competent layers and correspond to an asymmetrical internal boudinage (Cobbold *et al.* 1971), also known as extensional crenulation cleavage (Platt & Vissers 1980) and shear-band foliation (White *et al.* 1980); they require no further discussion here. The association of asymmetrical extensional shears with Type 2B pull-aparts and their analogues indicates a component of layer-parallel shear. However, Type 2A asymmetrical pull-aparts and foliation fish are clearly not analogous to either internal boudinage or extensional crenulation cleavage, since oblique extensional shears are absent.

Field kinematic context

The association of at least a component of layer-parallel shear with the formation of asymmetrical pull-aparts and foliation fish has been suggested in the foregoing paragraphs. Independent documentation and corroboration is provided by the consistency of the independent kinematic indicators in the field areas studied (Figs. 2b & c). Thus the following field-based kinematic implications are drawn with respect to the asymmetrical pull-aparts and foliation fish.

(i) The asymmetry of Type 1 asymmetrical pull-aparts is a direct reflection of the sense of non-coaxiality of the bulk deformation. Whereas in a coaxial deformation a symmetrical barrelling of initially rectangular boudins may result from internal ductile strain within the boudin (Ramberg 1955), in the non-coaxial case the highest strain rates are located in those corner volumes lying within the extensional field of the instantaneous strain ellipsoid.

(ii) The sense of asymmetry of Type 2 asymmetrical pull-aparts and foliation fish is antithetic to the sense of non-coaxiality of the bulk deformation. The 'swells' or ellipsoidal volumes of oblique internal foliation segments have rotated backwards. Indeed in one example presented, an independent indicator of bulk clockwise shear has been back-rotated in an anti-clockwise sense (Fig. 5b).

While these observations may appear intuitively obvious in the case of Types 1 and 2B structures (see Selkman 1978 and Platt & Vissers 1980), the common case of Type 2A structures and foliation fish requires further analysis before a comprehensive mechanical explanation of asymmetrical pull-aparts and their analogues can be attempted. To this end, the field observations and interpretations were tested by laboratory experiment.

EXPERIMENTAL STUDY

A hinged-frame shear box was used to impose a shear strain of 2.0 on a putty and Plasticine (McClay 1976) model (Fig. 6a). The apparatus comprised a number of aluminium plates, each cut to a shallow 'U'-shaped cross-section. The plates were stacked upright inside the hinged frame so as to present a concave-upward well to the camera. The model, 22 × 15 × 0.5 cm, sat flush within the well. By moving a side bar of the hinged frame, the aluminium plates were made to slide past each other and to transmit shear stresses to the model through the floor and the end-walls of the shear box. The deformation was performed by hand (at an approximate rate of displacement of 10^{-2} cm sec^{-1}).

The model comprised three layers of a competent material set in a matrix of silicone putty (Fig. 6a). The competent layers were all cut from a 5 mm thick Plasticine and silicone putty (1:2 ratio) multilayer. Individual layers within the multilayer were about 0.1 mm thick (Fig. 6c). A multilayer was chosen for the competent material for two reasons. (i) Many of the field examples of asymmetrical pull-aparts are multilayers. (ii) Attempts to construct the competent layers of an isotropic material only slightly stiffer than the silicone putty matrix by kneading the putty with Plasticine were unsuccessful on two counts. (a) It was difficult to ensure that the silicone putty/Plasticine mixes were truly isotropic. Despite prolonged kneading, an irregular streakiness was always apparent, suggesting the presence of a variably developed, indistinct layering. By creating a multilayer, the required competence was obtained and the layering was statistically homogeneous and unequivocal. (b) In a series of pilot experiments, 'isotropic' competent materials produced only subtle results after significant strain.

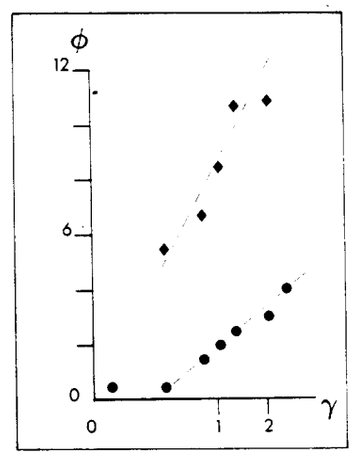

Fig. 7. Angle made by internal anisotropy with experimental bulk shear plane (ϕ) against shear strain (γ), recorded at intervals during the deformation. Mean synthetic (clockwise) rotation for eight corner volumes (top left and bottom right) of the four initial boudins in Type 1 asymmetrical pull-aparts (diamonds: five intervals). Mean antithetic (anti-clockwise) rotation for four 'swells' in Type 2 asymmetrical pull-aparts (dots: seven intervals). Dashed lines estimated by eye.

The competent material was installed in the model in three initial configurations in order to simulate a pre-experiment increment of finite strain. The configurations were (i) layers of initially symmetrical blocky boudins, (ii) thick pinch-and-swell structure and (iii) thin pinch-and-swell structure (Fig. 6a). The choice of initially symmetrical configurations requires some explanation, which I shall defer until the discussion section. The thin pinch-and-swell layer behaved as a passive marker (Ghosh & Ramberg 1976) and will not be discussed further (Fig. 6b). The initial boudins and 'swells' were constructed with similar 6:1 aspect ratios, the minimum required to inhibit rigid body rotation (Ghosh & Ramberg 1976). They were then inlaid such that each component of each competent layer, internal layering as well as the layers themselves, lay in the experimental bulk shear plane (Fig. 6a). The model was then left to sit and 'weld' for several hours prior to deformation in order to ensure maximum cohesion across the material contacts.

The results are presented in Figs. 6(b), (c) and 7. The initial rectangular grid and the boundaries of the model show that the deformation was homogeneous and that good cohesion was obtained throughout the model. The

top (free) surface of the model shows some mild deflections, especially in the immediate neighbourhood of the competent inclusions. These changes in free surface topography, while important enough to prohibit a detailed analysis of the local matrix flow adjacent to the inclusions, are of sufficiently minor amplitude to justify the assumption of homogeneous ideal simple shear boundary conditions for the bulk deformation.

Throughout the deformation, the internal layering and the long sides of the central parts of the individual blocky boudins remain sub-parallel to the bulk flow plane. The rotational component of the deformation, apparent from the shape of the deformed boudins, was therefore confined to the boudin extremities. Here, in the case of a sinistral shear, the top left and bottom right corner volumes of the boudins have flowed along anticlockwise deflecting particle paths towards the inter-boudin gaps. A similar response is barely perceptible in the other two corner volumes, so imparting an asymmetry ('Z' sigmoid shape) to the initially symmetrical boudins. The resultant structure is identical to field examples of Type 1 asymmetrical pull-aparts (compare Figs. 3b & c and 6b & c). The internal layering of the 'swells' of the pinch-and-swell structure shows no perceptible rotation with respect to the sides of the individual 'swells'. However, the individual 'swells' do show a pronounced and consistent back-rotation with respect to the sense of shear along the experimental flow plane. The resultant structure, given the lack of visible discrete extensional shears in the neck regions, is identical to field examples of Type 2A asymmetrical pull-aparts (compare Figs. 4a–c, 5 and 6b & c).

The deformed model was removed from the shear box, cut and re-inserted as a smaller plate. An additional shear strain of 0.75 was effected before boundary complications rendered the deformation inhomogeneous. These complications are due to the fact that, after cutting, the model no longer behaves as a thin plate and begins to buckle. The rotations of the internal layering and long sides of the boudin ends and of the long directions of the 'swells' are plotted for the complete experiment (Fig. 7). From this scant data, it would appear that the rotation rates are linear in both cases but that the synthetic rotation in the boudin corner volumes is more rapid than the antithetic rotation of the 'swells'.

DISCUSSION

An initially symmetrical configuration of blocky boudins and pinch-and-swell structure was built into the experimental model described above. It was chosen for its geometrical simplicity, but more especially because of the frequent association in the field of asymmetrical and symmetrical pull-apart structures. Asymmetrical and/or rotated boudins have been described elsewhere (e.g. Cloos 1947, Edelman 1949 p. 28, Ramberg 1955, De Sitter 1956 p. 88 and p. 308, Rast 1956, Sutton & Watson 1956, Coe 1959, Belousov 1962 p. 142 and p. 549, Uemura 1965, Paterson & Weiss 1968, Weiss 1972 fig. 145B, Dzis 1976), but only Strömgård (1973) attempted to rigorously address the question of their origin. Strömgård presented two models for the formation of primary asymmetrical boudins. The first is dependent upon stress refraction within multilayer systems and the assumption of boudinage by tensile failure. Strömgård demonstrated that because of the complex relationship between tensile local stresses, applied principal stress orientation and ratio, viscosity contrast and competent/incompetent layer thickness ratios, this model only produces markedly asymmetrical boudins at low confining pressures. Strömgård's second model is confining pressure independent and based upon consideration of finite strain and stress refraction in systems of low competent/incompetent layer thickness ratio, that is very widely spaced competent layers. Neither of these models is sufficiently general to account for the field examples presented here of asymmetrical boudins formed in close-spaced multilayers deformed at high metamorphic grade.

The selection of a symmetrical initial configuration in no way assumes a knowledge of the pre-experiment strain path or strain regime. The only assumptions are that, at some time prior to the (non-coaxial) finite strain increment under investigation, the direction of instantaneous maximum extension lay sub-parallel to the extended layer and that, at that time, the layer extended heterogeneously. Depending upon the rheological contrast with the matrix at the time, the competent layer is assumed to have boudinaged or to have developed a pinch-and-swell structure. Symmetrical heterogeneous extension of a competent layer does not, of itself, imply a coaxial strain history as Lister & Williams (1983) have clearly demonstrated. Furthermore, given the variable influence of the physico-chemical environment on the strengths of different minerals, the rheological contrast between the competent layer and its matrix may vary with metamorphic grade during syn-metamorphic deformation.

The model experiment of the present study strongly supports the field-based kinematic interpretation of the asymmetrical pull-apart structures and foliation fish outlined above. While this empirical support for the kinematic hypothesis is clear, a mechanical explanation of the observed flow is required.

Mechanical hypothesis

In the experiment described above, the model materials, the aspect ratios and the experimental conditions (e.g. strain rate) were identical for both the boudins and the pinch-and-swell structure. However, the initial geometrical configuration of the neck or inter-boudin regions is quite different in the two cases. The presence or absence of sharply defined corners determines which of the two principal physical properties (competence/viscosity and rheological anisotropy) of the boudins and pinch-and-swell structure is the predominant influence upon flow within the competent layers.

Type 1. The dynamic stress distribution in angular boudins is the result of two mutually dependent effects: (i) a geometrical stress-concentrator effect due to the presence of the sharp corners and (ii) a material stress-concentrator effect due to the competence/viscosity contrast between the boudin and its soft matrix. The dynamic stress distributions within blocky boudins subjected to a coaxial deformation are well documented (Stephansson & Berner 1971, Strömgård 1973, Selkman 1978, Lloyd & Ferguson 1981). The angular corner volumes are sites of anomalously high mean stress, while the inter-boudin gaps are sites of low mean stress. The ductile response of the boudin corner volumes to this mean stress gradient, that is flow towards the region of low mean stress, leads to the classical barrel shape of many boudins (Ramberg 1955). In the case of a layer-parallel shearing deformation, the existence of a shear stress along the boudin long-side will result in an asymmetrical stress distribution within the boudin such that maximum mean stresses will develop in those corner volumes lying within the extensional quadrants of the instantaneous strain ellipsoid (Selkman 1978, fig. 18). By analogy with symmetrical barrel-shaped boudins, Type 1 asymmetrical pull-aparts develop by flow of material from these sites of high mean stress towards the low pressure inter-boudin gaps.

Type 2A. Given the absence of sharply defined corners and of matrix-filled gaps between 'swells', the influence of competence/viscosity contrast on dynamic stress distribution within pinch-and-swell structure is attenuated. In other words, in the absence of geometrical stress concentrators, the distribution of mean stress is less heterogeneous within an individual 'swell' than in angular boudins. Therefore, the response to bulk shear is distributed throughout a given 'swell' and the influence of the internal rheological anisotropy on the flow pattern within the 'swell' is enhanced relative to that of competence/viscosity contrast. The following discussion also applies to the case of foliation fish.

The mechanical effect of a rheological anisotropy is to canalize and maximize slip along the anisotropy plane (Lister & Williams 1983). (In one of the pilot experiments, a passive grid of lines initially perpendicular to the internal anisotropy of the 'swells' was deflected by generally homogeneous slip on the internal layering). Consider a train of linked 'swells', similar to those of the experiment, whose principal planes are parallel to the bulk flow plane of a bulk ideal simple shear deformation. Let the orientation of the internal anisotropy deviate, slightly but randomly, from that of the bulk flow plane. There are three limiting cases, the first two of which are trivial:

(i) Within those 'swells' whose internal anisotropy lies in the bulk flow plane, slip on the anisotropy results in oblique extension of the 'swell', hence an apparent back-rotation of the principal plane of the 'swell', but no rotation of the internal anisotropy.

(ii) Within those 'swells' whose internal anisotropy lies within the shortening quadrants of the instantaneous strain ellipsoid, slip on the internal anisotropy, in combination with the resulting extension of the 'swells', produces an antithetic rotation of the internal anisotropy into the bulk flow plane (Hobbs *et al.* 1976, p. 124). The associated back-rotation of the principal plane of the 'swell' will be countered by its synthetic rotation with increasing finite strain.

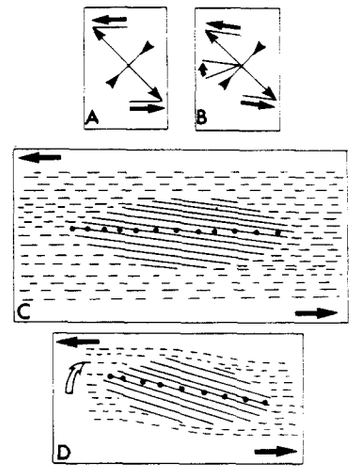

Fig. 8. Schematic representation of an initial perturbation in rheological anisotropy (e.g. mylonitic foliation) subjected to bulk ideal simple shear ($Sr = 0$) and lying in the extensional field of the bulk kinematic framework. (a) Bulk principal instantaneous stretches and shear plane are shown. (b) Because of the canalizing effect of the anisotropy with respect to slip, the local kinematic framework within the perturbation comprises slip along planes making an angle greater than 45 degrees to the bulk principal instantaneous shortening direction. The local strain regime therefore deviates from ideal simple shear such that $Sr > 0$. Under such conditions, there is a field of back-rotation as indicated by curved arrow. (c) and (d) The principal geometrical plane of the volume of perturbed anisotropy (dotted line) rotates antithetically with respect to the vorticity of the bulk imposed deformation. All angles grossly exaggerated.

(iii) Within those 'swells' whose internal anisotropy lies in the extensional quadrants of the instantaneous strain ellipsoid, the deformation deviates from ideal simple shear such that the strain rate ratio (Sr = pure shear strain rate/simple shear strain rate) is greater than zero (Fig. 8). Because of the good 'swell'–matrix cohesion, this deviation will extend a short distance into the surrounding incompetent matrix (contact strain area of Ramsay 1967, p. 416). Ghosh & Ramberg (1976) have demonstrated that for such strain rate ratios, a field of back-rotation is generated whose bisector lies within the shortening quadrants of the instantaneous strain ellipsoid and makes an acute angle with the plane of shear (Fig. 8). This angle and the field width are proportional to the strain rate ratio. Applying Ghosh & Ramberg's analysis to the experiment described here, during the first increment of bulk simple shear affecting such an initial configuration, the principal plane of the 'swell' lies within the field of back-rotation generated by the flow in its own matrix envelope (Fig. 8). Back-rotation of the principal plane and therefore of the internal anisotropy further accentuates the deviation from ideal simple shear (increases the strain rate ratio) within and about the 'swell'. The process is, however, self regulating since

back-rotation leads to a hardening of the internal anisotropy with respect to slip. When hardening is sufficiently advanced, the deviation from ideal simple shear in the enveloping matrix will attenuate and the 'swell' will tend to rotate synthetically in response to continuing bulk simple shear, so softening the internal anisotropy with respect to slip. Field observation suggests empirically that back-rotation is balanced by rotational hardening after antithetic rotation of the order of 10–15 degrees.

Type 2B. The back-rotation of the 'swells' between discrete extensional shears may be expressed as the flow resulting from the following boundary conditions imposed by the slip on the asymmetrical extensional shears and the initial orientation of the principal plane of the 'swells' in the direction of the bulk flow plane of the deformation.

(i) The ends of the 'swells' are offset by a shear couple synthetic to the sense of shear on the bulk layering (bulk flow plane).

(ii) The plane containing the centres of the initial individual 'swells' cannot rotate through the bulk flow plane.

The result must be the back-rotation of the 'swells' with progressive shear (see Platt & Vissers 1980).

A cautionary note

As with all kinematic indicators, there are limitations to the use of the structures discussed herein. Apart from the obvious relationship between the scale of observation and that of the interpretation (Schwerdtner 1973, Hanmer 1982), it is for the observer to ensure that consistent observations are sufficiently numerous (e.g. trains of asymmetrical boudins or 'swells') to allow reasonable inference of a systematic asymmetry. As with all kinematic indicators, Types 1 and 2 asymmetrical pull-aparts and foliation fish should be used as components of structural assemblages of mechanically independent kinematic indicators from which to interpret the kinematic significance of the deformation (Hanmer 1984a).

CONCLUSIONS

(1) Shearing along a plane containing blocky boudins (initially symmetrical in this analysis) can produce asymmetric barrelling simply related to the shear sense of the bulk flow (Type 1 asymmetrical pull-aparts).

(2) Shearing along a plane containing pinch-and-swell structure (initially symmetrical and internally anisotropic in this analysis) can produce an antithetic rotation of the 'swells'. This back-rotation is either a response to slip along the internal anisotropy and local deviation from ideal simple shear ($Sr > 0$: Type 2A asymmetrical pull-aparts) or a response to displacement along discrete asymmetrical extensional shears located between the 'swells' (Type 2B). The two idealized responses are not mutually exclusive.

(3) In the presence of the geometrical stress concentration effect of the angular corners, competence/viscosity controls the response of the boudins to shear (Type 1). In the absence of angular corners, internal anisotropy controls the response of the pinch-and-swell structures to shear (Type 2A).

(4) Structures which are geometrically and mechanically analogous to Type 2 asymmetrical pull-aparts can form in the absence of competent layers in well foliated rocks. Such analogues of Type 2A structures are called foliation fish.

(5) Asymmetrical pull-aparts and foliation fish formed by the mechanisms proposed in this paper are indicators of shear sense which can be used in the field as components of an assemblage of mechanically independent kinematic indicators to determine the vorticity of non-coaxial flow in ductile tectonites.

Acknowledgements—This paper was presented orally at the International Conference on Tectonic and Structural Processes held at Utrecht University, the Netherlands, 10–12 April 1985 (Hanmer 1985). The experimental work for this study was carried out using equipment and materials of the Structural Geology Laboratory at Queen's University, Kingston, Ontario. I am most grateful to John Dixon and John Summers for their hospitality and their advice in building the models. I thank them both as well as Win Means, Rein Tirrul and Paul Williams for critically reading an earlier draft of this paper. The manuscript was improved by constructive reviews by Jean-Pierre Burg and an anonymous reviewer. All errors of interpretation remain my own. Bev Cox tirelessly typed the several versions of the manuscript.

REFERENCES

Beloussov, V. V. 1962. *Basic problems in Geotectonics*. McGraw-Hill, New York.

Berthé, D., Choukroune, P. & Jegouzo, P. 1979. Orthogneiss, mylonite and non-coaxial deformation of granites: the example of the South Armoricain shear zone. *J. Struct. Geol.* **1**, 31–42.

Bruhl, H. 1967. Boudinage als Ergbnis der inneren Deformation. *Geol. Mitt.* **8**, 263–308.

Burg, J. P. & Harris, L. B. 1982. Tension fractures and boudinage oblique to the maximum extension direction: an analogy with Lüders' bands. *Tectonophysics* **83**, 347–363.

Cloos, H. 1947. Boudinage. *Trans. Am. geophys. Un.* **28**, 626–632.

Cobbold, P. R., Cosgrove, J. W. & Summers, J. M. 1971. Development of internal structures in deformed anisotropic rocks. *Tectonophysics* **12**, 23–53.

Coe, K. 1959. Boudinage structure in West Cork, Ireland. *Geol. Mag.* **96**, 191–200.

Corin, F. 1931. A propos du boudinage en Ardenne. *Bull. Soc. belge Géol. Paléont. Hydrol.* **42**, 101–117.

Culshaw, N. G., Davidson, A. & Nadeau, L. 1983. Structural subdivisions of the Grenville Province in the Parry Sound–Algonquin region, Ontario. *Curr. Res. Geol. Surv. Pap. Can.* **83-1B**, 243–252.

Davidson, A., Culshaw, N. G., & Nadeau, L. 1982. A tectonometamorphic framework for part of the Grenville Province, Ontario. *Curr. Res. Geol. Surv. Pap. Can.* **82-1A**, 175–190.

Dearman, W. R. 1966. Mullion and boudinage structure in Coryston slate quarry near Okehampton, Devonshire. *Geol. Mag.* **103**, 204–213.

De Sitter, L. U. 1956. *Structural Geology*. McGraw-Hill, New York.

Durney, D. W. & Ramsay, J. G. 1973. Incremental strains measured by syntectonic crystal growths. In: *Gravity and Tectonics* (edited by DeJong, K. A. & Scholten, R.). Wiley, New York.

Dzis, R. J. 1976. Finite and incremental deformations recorded by planar subfabrics and S tectonites. *Tectonophysics* **36**, 367–393.

Edelman, N. 1949. Structural history of the eastern part of the Gulkrona basin, S.W. Finland. *Bull. Comm. geol. Finl.* **148**, 1–87.

Fullagar, P. K. 1980. A description of nucleation of folds and boudins in terms of vorticity. *Tectonophysics* **65**, 39–55.

Ghosh, S. K. & Ramberg, H. 1976. Reorientation of inclusions by

combination of pure shear and simple shear. *Tectonophysics* **34**, 1–70.

Hanmer, S. 1982. Vein arrays as kinematic indicators in kinked anisotropic materials. *J. Struct. Geol.* **4**, 151–160.

Hanmer, S. 1984a. Strain insensitive foliations in polymineralic rocks. *Can. J. Earth Sci.* **21**, 1410–1414.

Hanmer, S. 1984b. The potential use of planar and elliptical structures as indicators of strain regime and kinematics of tectonic flow. *Curr. Res. Geol. Surv. Pap. Can.* **84-1B**, 133–142.

Hanmer, S. 1985. Potential kinematic model for some natural and experimental asymmetrical pull-apart structures. Int. Conf. on Tectonic and Struct. Processes, 10–12 April, Utrecht. Abstract, 33.

Hanmer, S. & Ciesielski, A. 1984. A structural reconnaissance of the northwest boundary of the Central Metasedimentary Belt, Grenville Province, Ontario and Québec. *Curr. Res. Geol. Surv. Pap. Can.* **84-1B**, 121–131.

Hanmer, S. & Lucas, S. B. 1985. Anatomy of a ductile transcurrent shear; the Great Slave Lake Shear Zone, District of Mackenzie, N.W.T. (Preliminary Report). *Curr. Res. Geol. Surv. Pap. Can.* **85-1B**,7–22.

Hanmer, S., Thivierge, R. H. & Henderson, J. R. 1985. Anatomy of a ductile thrust zone: part of the boundary of the Central Metasedimentary Belt, Grenville Province, Ontario. *Curr. Res. Geol. Surv. Pap. Can.* **85-1B**, 1–5.

Harker, A. 1889. On the local thickening of beds by folding. *Geol. Mag.* **6**, 69–70.

Hobbs, B. E., Means, W. D. & Williams, P. F. 1976. *An Outline of Structural Geology*. Wiley & Sons.

Holmquist, P. J. 1931. On the relations of the boudinage structure. *Geol. För. Stockh. Förh.* **53**, 193–208.

Lister, G. S. & Price, G. P. 1978. Fabric development in a quartz–feldspar mylonite. *Tectonophysics* **49**, 37–78.

Lister, G. S. & Williams, P. F. 1983. The partitioning of deformation in flowing rock masses. *Tectonophysics* **92**, 1–33.

Lloyd, G. E. & Ferguson, C. C. 1981. Boudinage structures: some new interpretations based on elastic-plastic finite element simulations. *J. Struct. Geol.* **3**, 117–128.

Lloyd, G. E., Ferguson, C. C. & Reading, K. 1982. A stress transfer model for the development of extension fracture boudinage. *J. Struct. Geol.* **4**, 355–372.

Lohest, M. 1909. De l'origine des veines et des géodes des terrains primaires de Belgique. *Ann. Soc. géol. Belg.* **36B**, 275–282.

McClay, K. R. 1976. The rheology of plasticine. *Tectonophysics* **33**, T7–T15.

Means, W. D. 1981. The concept of steady-state foliation. *Tectonophysics* **78**, 179–199.

Means, W. D., Hobbs, B. E., Lister, G. S. & Williams, P. F. 1980. Vorticity and non-coaxiality in progressive deformations. *J. Struct. Geol.* **2**, 371–378.

Neurath, C. & Smith, R. B. 1982. The effect of material properties on growth rates of folding and boudinage: experiments with wax models. *J. Struct. Geol.* **4**, 215–299.

Paterson, M. S. & Weiss, L. E. 1968. Folding and boudinage of quartz-rich layers in experimentally deformed phyllite. *Bull. geol. Soc. Am.* **79**, 795–812.

Platt, J. P. & Vissers, R. L. 1980. Extensional structures in anisotropic rocks. *J. Struct. Geol.* **2**, 397–410.

Quirke, T. T. 1923. Boudinage: an unusual structural phenomenon. *Bull. geol. Soc. Am.* **34**, 649–660.

Ramberg, H. 1955. Natural and experimental boudinage and pinch-and-swell structures. *J. Geol.* **63**, 512–526.

Ramsay, J. G. 1967. *Folding and Fracturing of Rocks*. McGraw-Hill, New York.

Ramsay, J. G. & Graham, R. H. 1970. Strain variation in shear belts. *Can. J. Earth Sci.* **7**, 786–813.

Rast, N. 1956. The origin and significance of boudinage. *Geol. Mag.* **93**, 401–408.

Reches, Z. & Johnson, A. M. 1976. A theory of concentric kink and sinusoidal folding and of monoclinal flexuring of compressible elastic multilayers. *Tectonophysics* **35**, 295–334.

Reinhardt, E. W. 1969. Geology of the Precambrian rocks of Thubun Lakes map area in relationship to the McDonald Fault System, District of Mackenzie. *Geol. Surv. Pap. Can.* **69-21**, 1–29.

Rosenfeld, J. L. 1970. Rotated garnets in metamorphic rocks. *Spec. Pap. geol. Soc. Am.* **129**.

Sanderson, D. J. 1974. Patterns of boudinage and apparent stretching lineation developed in folded rocks. *J. Geol.* **82**, 651–661.

Schwerdtner, W. M. 1973. A scale problem in paleo-strain analysis. *Tectonophysics*, **16**, 47–54.

Selkman, S. 1978. Stress and displacement analysis of boudinage by the finite element method. *Tectonophysics* **44**, 115–139.

Simpson, C. 1983. Strain and shape-fabric variations associated with ductile shear zones. *J. Struct. Geol.* **5**, 61–72.

Smith, R. B. 1975. Unified theory for the onset of folding, boudinage and mullion structure. *Bull. geol. Soc. Am.* **86**, 1601–1609.

Smith, R. B. 1977. Formation of folds, boudinage and mullions in non-Newtonian materials. *Bull. geol. Soc. Am.* **88**, 312–320.

Stephansson, O. & Berner, H. 1971. The finite element method in tectonic processes. *Phys. Earth Plant. Int.* **4**, 301–321.

Strömgård, K. E. 1973. Stress distribution during deformation of boudinage and pressure shadows. *Tectonophysics* **16**, 215–248.

Sutton, J. & Watson, J. 1956. The Boyndie syncline of the Dalradian of the Banffshire coast. *Q. Jl geol. Soc. Lond.* **112**, 103–130.

Talbot, C. J. 1970. The minimum strain ellipsoid using quartz veins. *Tectonophysics* **9**, 47–76.

Uemura, T. 1965. Tectonic analysis of the boudin structure in the Muro group, Kii Peninsula, southwest Japan. *J. Earth Sci. Nagoya Univ.* **13**, 99–114.

Wegmann, C. E. 1932. Note sur le boudinage. *Bull. Soc. géol. Fr.* **2**, 477–491.

Weiss, L. E. 1972. *The Minor Structures of Deformed Rocks*. Springer, Berlin.

White, S. H., Burrows, S. E., Carreras, J., Shaw, N. & Humphreys, F. J. 1980. On mylonites in ductile shear zones. *J. Struct. Geol.* **2**, 175–188.

Wilson, G. 1982. *Introduction to Small-scale Geological Structures*. Allen & Unwin.

Wynne-Edwards, H. R. 1972. The Grenville province. In: *Variations in Tectonic Styles in Canada* (edited by Price, R. A. & Douglas, R. J. W.), *Spec. Pap. Geol. Ass. Can.* **11**, 263–334.